Structure of UDP-*N*-acetylglucosamine enolpyruvyl transferase, an enzyme essential for the synthesis of bacterial peptidoglycan, complexed with substrate UDP-*N*-acetylglucosamine and the drug fosfomycin

Tadeusz Skarzynski*, Anil Mistry†, Alan Wonacott, Susan E Hutchinson, Valerie A Kelly and Kenneth Duncan

Background: UDP-*N*-acetylglucosamine enolpyruvyl transferase (MurA), catalyses the first committed step of bacterial cell wall biosynthesis and is a target for the antibiotic fosfomycin. The only other known enolpyruvyl transferase is 5-enolpyruvylshikimate-3-phosphate (EPSP) synthase, an enzyme involved in the shikimic acid pathway and the target for the herbicide glyphosate. Inhibitors of enolypyruvyl transferases are of biotechnological interest as MurA and EPSP synthase are found exclusively in plants and microbes.

Results: The crystal structure of *Escherichia coli* MurA complexed with UDP-*N*-acetylglucosamine (UDP-GlcNAc) and fosfomycin has been determined at 1.8 Å resolution. The structure consists of two domains with the active site located between them. The domains have a very similar secondary structure, and the overall protein architecture is similar to that of EPSP synthase. The fosfomycin molecule is covalently bound to the cysteine residue Cys115, whereas UDP-GlcNAc makes several hydrogen-bonding interactions with residues from both domains.

Conclusions: The present structure reveals the mode of binding of the natural substrate UDP-GlcNAc and of the drug fosfomycin, and provides information on the residues involved in catalysis. These results should aid the design of inhibitors which would interfere with enzyme-catalyzed reactions in the early stage of the bacterial cell wall biosynthesis. Furthermore, the crystal structure of MurA provides a model for predicting active-site residues in EPSP synthase that may be involved in catalysis and substrate binding.

Address: Glaxo Wellcome Research and Development, Medicines Research Centre, Gunnels Wood Road, Stevenage, SG1 2NY, UK.

†Present address: Zeneca Pharmaceuticals, Alderley Park, Macclesfield, SK10 4TG, UK.

*Corresponding author.
E-mail: ts14913@ggr.co.uk

Key words: enolpyruvyl transferase, fosfomycin, peptidoglycan biosynthesis, substrate binding, X-ray crystallography

Received: 15 August 1996
Revisions requested: 10 September 1996
Revisions received: 25 September 1996
Accepted: 26 September 1996

Structure 15 December 1996, 4:1465–1474

Introduction

Peptidoglycan is an extensively cross-linked polymer essential for the integrity of the bacterial cell wall. Many antibiotics act by disruption of its biosynthesis and assembly, several are targeted against the cytoplasmic enzymes that synthesise the key intermediate UDP-*N*-acetylmuramyl pentapeptide [1]. One such drug is fosfomycin (phosphonomycin, (1R,2S)-1,2-epoxypropylphosphonic acid) [2,3], which inactivates the first enzyme in this pathway, UDP-*N*-acetylglucosamine enolpyruvyl transferase (MurA; E.C. 2.5.1.7, alternative name UDP-*N*-acetylglucosamine 1-carboxyvinyltransferase). The emergence of bacterial strains resistant to this and to other antibiotics has focused attention on the need to constantly improve our armament of antibacterial agents. Detailed study of the reaction mechanisms of several enzymes in the UDP-*N*-acetylmuramyl pentapeptide pathway, including MurA, has provided strategies for the rational design of novel inhibitors, a process aided by the availability of crystal structures of three enzymes, UDP-*N*-acetylenolpyruvyl-glucosamine reductase [4], D-Alanine:D-Alanine ligase [5] and UDP-*N*-acetylmuramate-L-alanine ligase [6].

The *Enterobacter cloacae* [7] and *Escherichia coli* [8] *murA* genes have been cloned, sequenced, and coupled to powerful expression systems in order to overproduce large amounts of the protein in *E. coli*. In each case, MurA activity was shown to reside on a single monomeric polypeptide chain corresponding to the molecular mass predicted from the gene sequence. Homologous genes have been identified in a diverse range of bacterial species, including *Mycobacterium tuberculosis* ([9]; KE Kempsell and KD, unpublished data), *Mycobacterium leprae* [10], *Haemophilus influenzae* [11], *Bacillus subtilis* [12] and *Acinetobacter calcoaceticus* [13].

There are only two known enolpyruvyl transferases, MurA and 5-enolpyruvyl-shikimate-3-phosphate (EPSP) synthase, an enzyme in the shikimic acid pathway leading to the precursor of aromatic compounds in plants and microbes,

Figure 1

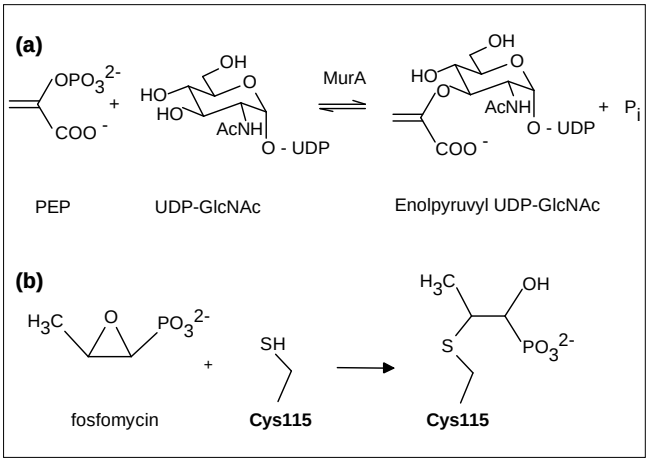

(a) The enolpyruvyl transfer reaction catalyzed by MurA. (b) The reaction between fosfomycin and Cys115 of MurA, which results in inactivation of the enzyme.

chorismic acid. MurA and EPSP synthase share low-level amino acid sequence similarity (about 20% identity for enzymes from *E. coli* [8,14]), but greater similarity at the structural level was suggested by the presence of a repeating motif at similar positions in both sequences [8]. The crystal structure of a substrate-free form of EPSP synthase has been determined at 2.5 Å [15], revealing a distinctive two-domain structure. However, it does not provide information on the residues that may be involved in substrate binding and catalysis. The reaction catalyzed by MurA (Fig. 1a) proceeds via an addition–elimination mechanism [16], analogous to that catalyzed by EPSP synthase [17–19]. A noncovalently-bound tetrahedral ketal intermediate is formed by direct attack of the 3′-OH of UDP-*N*-acetylglucosamine (UDP-GlcNAc) on the C-2 position of phosphoenolpyruvate (PEP), inorganic phosphate is then eliminated to form the product, UDP-*N*-acetylenolpyruvylglucosamine. Purified MurA from *E. coli* and *E. cloacae* has a molecule of PEP bound to Cys115 which suggests that the mechanism proceeds via a phospholactyl enzyme intermediate [20–22]. However, by analysing the *E. coli* MurA with a Cys115→Asp115 mutation, it was concluded that covalently bound PEP is not essential for catalysis [23]. In addition, there is no evidence for cysteine involvement in the EPSP synthase mechanism. Each enzyme is exquisitely sensitive to different inhibitors: MurA to the antibiotic fosfomycin, which binds covalently via a thioether bond to Cys115 [3,24] (Fig. 1b); and EPSP synthase to the herbicide glyphosate (*N*-(phosphonomethyl)glycine) [25].

We have determined the three-dimensional structure of *E. coli* MurA complexed with UDP-GlcNAc and fosfomycin, at 1.8 Å resolution. This report describes the structure, compares it with that of EPSP synthase, and presents details of protein–substrate interactions.

Results and discussion

Structure determination and refinement

The structure of MurA complexed with UDP-GlcNAc and fosfomycin was solved by multiple isomorphous replacement (MIR) at 3.2 Å resolution and refined at 1.8 Å resolution. Crystals, grown from *tert*-butanol solutions, were very unstable at room temperature, and X-ray data collection was only possible using flash-frozen crystals maintained at 100 K. A search for heavy-atom derivatives yielded three useful derivatives: chloro (2,2′:6′2″-terpyridine) platinum (II), potassium hexachloroplatinate and potassium tetrachloroplatinate. Diffraction data for the derivatives extended to 3.0 Å, but only produced useful phasing information to about 3.2 Å (Table 1), which resulted in electron-density maps that were difficult to interpret. Several

Table 1

Crystallographic data.

	Data set					
	Native 1	Native 2	TP10	TP25	PTCL	PT04
Resolution (Å)	2.7	1.8	2.8	3.0	2.9	2.8
Complete (%)	95	95	98	98	92	93
R_{merge}*	0.105	0.080	0.098	0.113	0.100	0.081
MIR phasing						
R_{iso}†			0.300	0.146	0.202	0.164
No. of sites			4	2	1	1
Resolution cut-off (Å)			3.2	3.2	3.2	4.0
R_{cullis}‡ (centric data)			0.70	0.82	0.88	0.83
Phasing power			1.37	0.91	0.79	0.86

Mean figure of merit = 0.47. Heavy-atom derivatives: TP10: chloro (2,2′:6′2″-terpyridine) platinum (II), saturated solution; TP25: chloro (2,2′:6′2″-terpyridine) platinum (II), 25% saturated; PTCL: K_2PtCl_6, saturated; PT04: K_2PtCl_4, 10 mM. *$R_{merge} = \Sigma_{hkl}\Sigma_i|I - \langle I \rangle|/\Sigma_{hkl}\Sigma_i I$.
†$R_{iso} = \Sigma_{hkl}|(F_{PH} - Fp|/\Sigma_{hkl}F_P$.
‡$R_{cullis} = \Sigma_{hkl}||F_{PH} \pm F_P| - F_H(calc)|/\Sigma_{hkl}|F_{PH} \pm F_P|$.

Figure 2

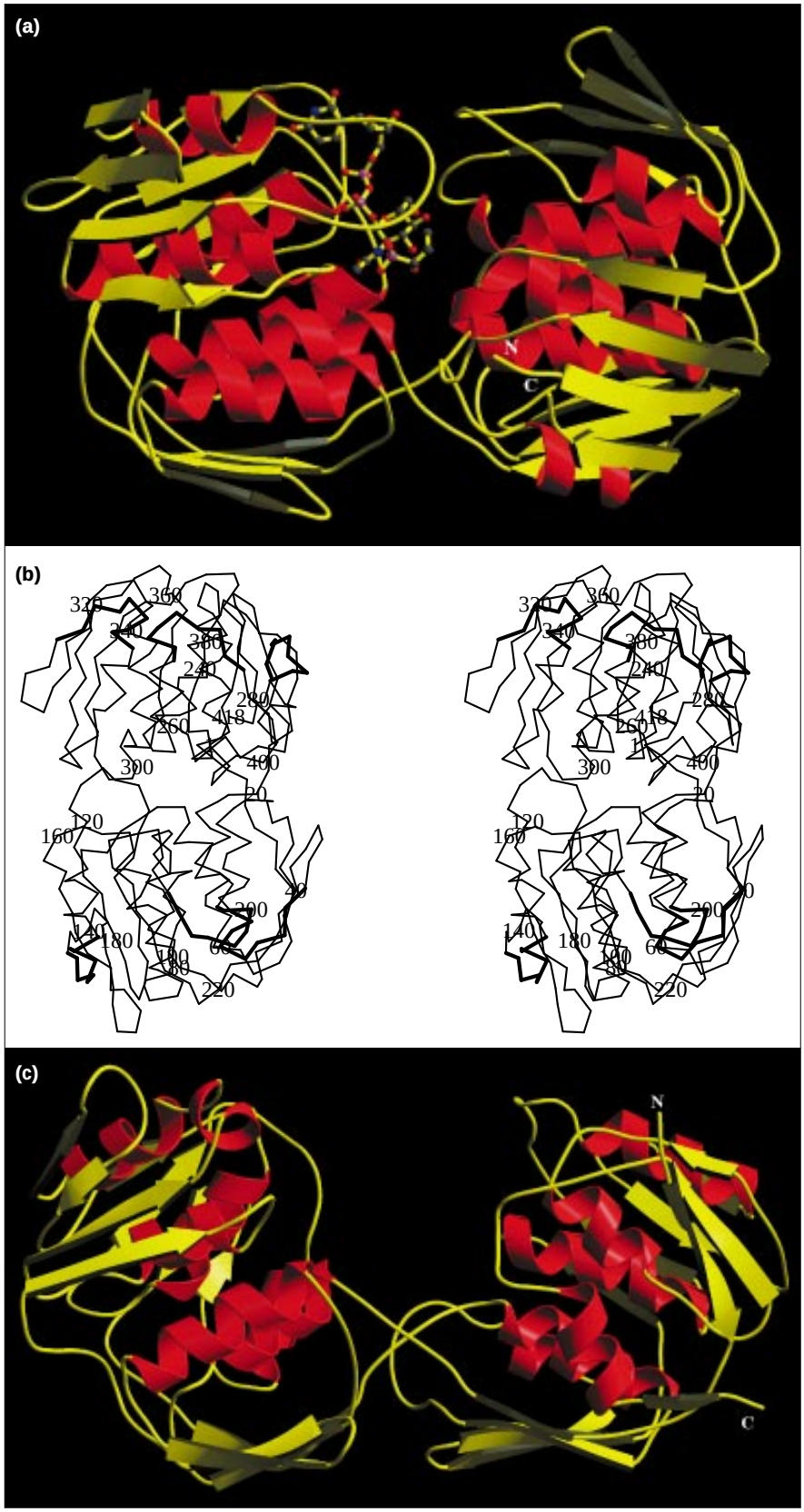

The mainchain fold of enolpyruvyl transferases. (a) A schematic representation of the MurA structure, showing the overall protein architecture, with the ball-and-stick model representing UDP-GlcNAc and fosfomycin molecules bound in the active site. (b) Stereo representation of the α-carbon backbone of MurA with every 20th residue labelled. Thick lines correspond to the conserved motif Leu-X-X-Leu-Gly-Ala-polar-hydrophobic-polar (see text). The molecule is rotated anticlockwise by 90° relative to (a). (c) A ribbon representation of EPSP synthase based on the Brookhaven Protein Data Bank entry 1EPS. In (a) and (c) α-helical regions are coloured in red. The figure was generated using the programs MOLSCRIPT [38] and RASTER3D [39,40].

density modification, phase extension and model rebuilding rounds were performed, resulting in the complete determination of the protein structure with the exception of the C-terminal residue Glu419, which cannot be seen in the electron-density map. A difference electron-density map computed after initial refinement of the atomic coordinates for the protein clearly showed an outline of the UDP-GlcNAc and fosfomycin molecules in the active site. High-resolution X-ray data collected to 1.8 Å resolution using synchrotron radiation were subsequently used in the refinement of the structure. The refined structure includes 418 residues, UDP-GlcNAc and fosfomycin, and 422 water molecules. The final crystallographic R factor is 0.185 for all data in the resolution range of 6.0 and 1.8 Å.

Overall structure

MurA has two globular domains connected by a double-stranded linker (Fig. 2a). In this report, the domain containing the catalytic Cys115 (residues 22–229) will be termed the catalytic domain, and the other domain (residues 1–21 and 230–419) will be called the C-terminal domain. The mainchain fold of each domain is very similar, with three parallel internal helices surrounded by three helices and three four-stranded β-sheets exposed to solvent. There is an approximate threefold symmetry which relates secondary structure elements within each of the domains. Marquardt *et al.* [8] suggested that the MurA sequence may be divided into six units of approximately 70 residues, each containing a conserved motif, Leu-X-X-Leu-Gly-Ala-polar-hydrophobic-polar. In the crystal structure of MurA, this conserved motif corresponds to the arrangement involving the C-terminal end of the exposed helix, a connecting loop and the N-terminal end of the first strand in the adjacent β sheet (Fig. 2b).

Comparison of the MurA and EPSP synthase structures

The overall protein fold is very similar to that of EPSP synthase [15] (Fig. 2c), although several loops connecting the secondary structure elements differ in length and conformation. The relative orientation of the domains differs significantly; in EPSP synthase, the enzyme is in an 'open' conformation with an empty active site, whereas MurA is in a 'closed' conformation, with the two domains enveloping substrate and inhibitor. In MurA, the loop 111–121 has an extended conformation, creating a 'lid' over the catalytic pocket, whereas the corresponding stretch of the EPSP synthase polypeptide chain forms a short helix. In MurA, there are glycine residues at both ends of the loop 111–121, and it is very likely that the conformation of this solvent-exposed part of the molecule is different in an open form. Several other loops near the active-site pocket vary in length and conformation in the two enzymes (Fig. 2).

The MurA and EPSP synthase structures also differ in the length and relative orientation of individual β strands and helices. For example, the C-terminal strand in MurA belongs to the 'four-β-strand, two-α-helix' motif, repeated six times in the structure of the enzyme, while in EPSP synthase the polypeptide chain ends somewhat earlier, and the fourth β strand of the motif is missing. Stallings *et al.* [15] suggested that the topological symmetry of EPSP synthase may reflect sixfold gene replication. They also

Figure 3

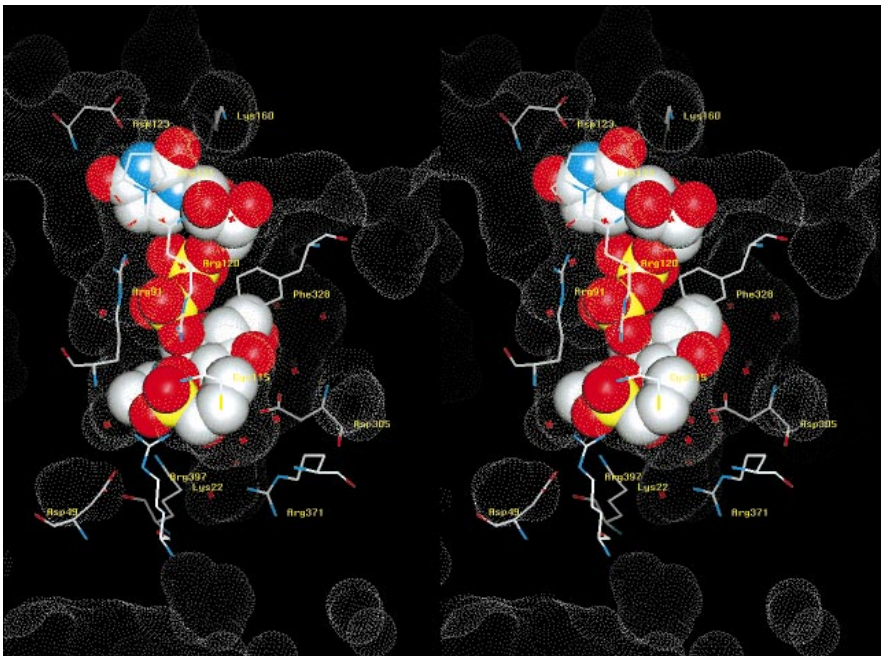

A stereo representation of the active site of MurA with a cross-section through the molecular surface of the enzyme (white dots) showing surface complementarity between the ligands and the protein (stick representation). UDP-GlcNAc and fosfomycin are represented as van der Waals spheres. Atoms are depicted in standard colours. Only residues mentioned in the text are shown, along with water molecules (represented as red crosses) trapped in the catalytic pocket. Figure was produced with the program QUANTA (Molecular Simulations Inc.).

noted that the arrangement of the 12 helices in EPSP synthase, with their N termini pointing towards the active site, may favour the binding of negatively charged ligands. The similar arrangement of the helices in MurA suggests that it may have a similar role in binding of the negatively-charged substrates UDP-GlcNAc and PEP.

The catalytic site

The catalytic site is situated in a deep cavity between the two domains (Fig. 3). There are 10 direct interdomain hydrogen bonds involving residues distributed around the catalytic pocket. These include four hydrogen bonds between loops 46–49 and 396–400 (including the salt bridge Asp49–Arg397), three hydrogen bonds between the loops 116–119 and 329-330, a hydrogen bond between Glu188 and His299, and two hydrogen bonds (a salt bridge) between Glu190 and Arg232 at the bottom of the active-site cavity. There are no large hydrophobic patches buried between the domains and only a few hydrophobic interactions between single residues can be found in the interface (e.g. Ile117–Phe328 and Val161–Pro298). The interdomain interactions stabilise the closed conformation of the enzyme, but may also play a more specific role in catalysis, by controlling access to the active site at different stages of the reaction. For example, the salt bridge between Asp49 and Arg 397 (both residues conserved in all known MurA sequences) is positioned between the active site and the bulk solvent, with the arginine contributing to the phosphate-binding site (see further below).

Interactions between MurA and UDP-GlcNAc

The uridinyl ring of UDP-GlcNAc is sandwiched between two hydrophobic surfaces created by Arg120 and Pro121 on one face and Leu124 on the other, ensuring a good fit of the molecular surfaces (Fig. 3). These interactions, combined with the hydrogen bonds involving uridinyl base atoms N1 and O1, provide good binding specificity for this base. There is less surface complementarity between the *N*-acetylglucosamine moiety and the protein. The sugar rests against one side of the active site pocket and interacts with a number of water molecules trapped there; it makes three hydrogen bonds with the protein involving Asn23 (one bond) and Asp305 (two bonds) from the C-terminal domain (Fig. 4). The principal substrate-binding interactions involve oxygen atoms from the pyrophosphate bridge of UDP-GlcNAc, which make hydrogen bonds to two mainchain nitrogen atoms of Val163 and Gly164, a hydrogen bond with the hydroxyl oxygen of Ser162, and two hydrogen bonds with arginine residues Arg91 and Arg120 (Fig. 4).

There are several pools of buried solvent molecules. Between UDP-GlcNAc and the C-terminal domain of the enzyme, a cluster of three water molecules fills a cavity at the bottom of the active site. A chain of water molecules creates a narrow channel in the C-terminal domain between the ribose ring of UDP-GlcNAc and the exposed surface of the protein, close to helix 260–269 and loop 298–304. Water molecules fill small cavities near the *N*-acetylglucosamine moiety. There is a distinctive cleft on the surface of the catalytic domain, surrounding most of the substrate-binding site, whose charge distribution is complementary to that of the substrate (Fig. 5). The shape complementarity, and the specific protein–ligand interactions between UDP-GlcNAc and the catalytic domain, indicate this cleft may be the likely site of initial substrate recognition and binding to the open form of the protein.

Figure 4

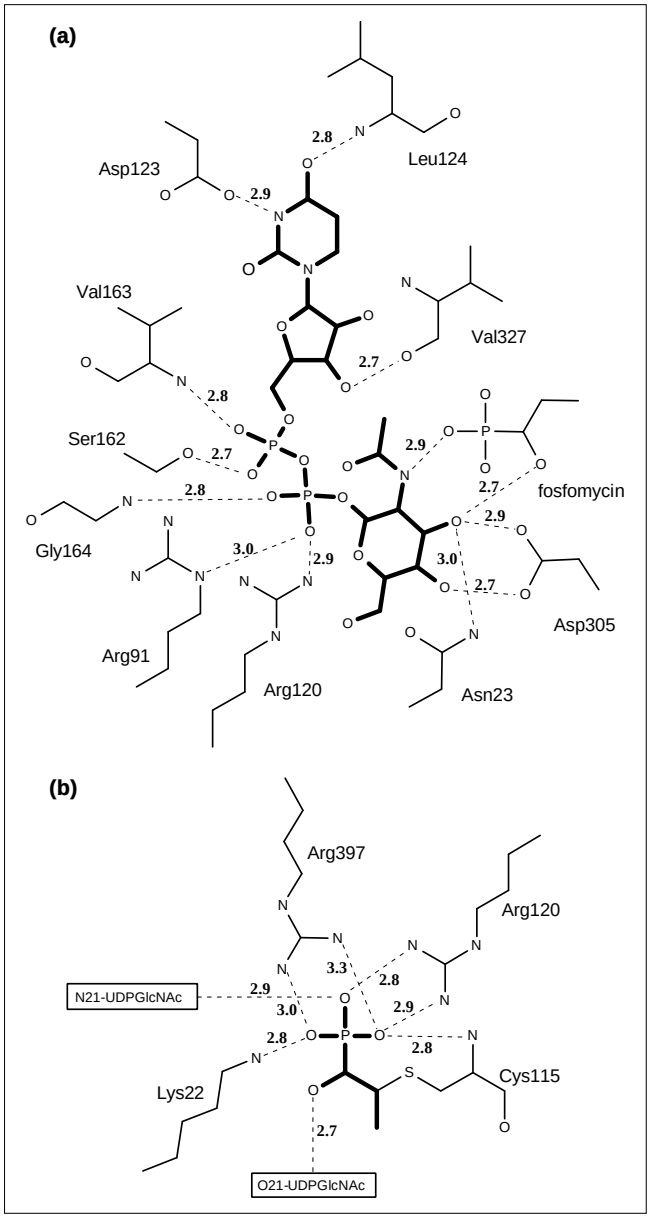

A schematic diagram of hydrogen bonds made by (a) UDP-GlcNAc and (b) fosfomycin with residues of MurA (thin lines). Residues of both ligands are shown as thick lines. Hydrogen bonds are denoted as dashed lines.

Figure 5

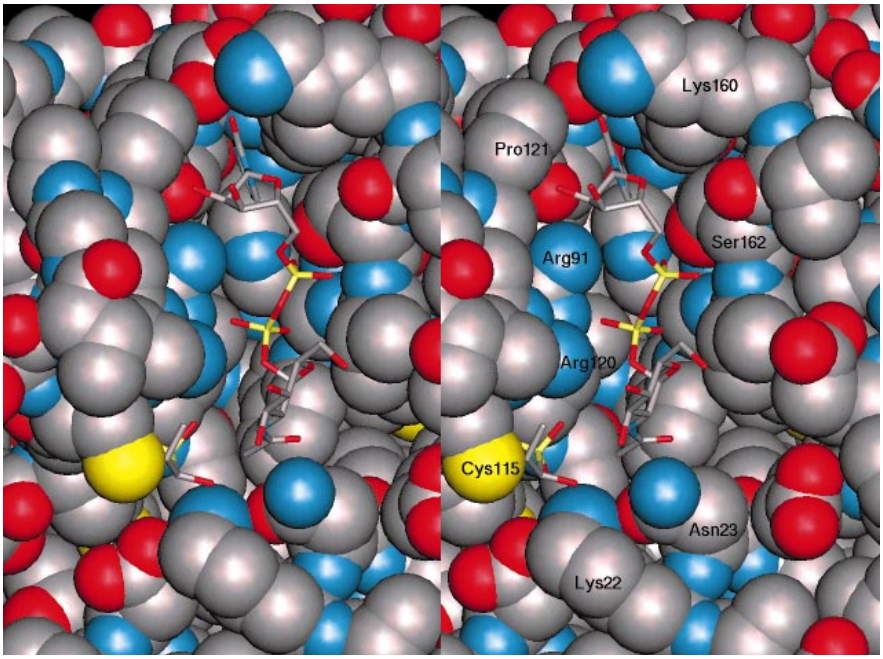

A stereo representation of the cavity in the catalytic domain of MurA surrounding the UDP-GlcNAc and fosfomycin molecules (represented by stick models). Protein atoms are shown as van der Waals spheres. Nitrogen atoms are coloured in blue, oxygen atoms in red, the sulphur atom of Cys115 in yellow. The C-terminal domain and water molecules are not shown. Figure was produced with the program QUANTA (Molecular Simulations Inc.).

Interactions between MurA and fosfomycin

Fosfomycin is tightly packed between the enzyme and UDP-GlcNAc (Figs 3,5), making hydrogen bonds with several different segments of the polypeptide chain (Fig. 4b). There are also hydrogen bonds between the fosfomycin hydroxyl group and the C-3 hydroxyl of the UDP-GlcNAc sugar ring, and between one of its phosphonate oxygen atoms and the amide nitrogen of UDP-GlcNAc (Fig. 4a). Three positively charged residues of MurA (Lys22, Arg120 and Arg397) surround the phosphonate group, providing strong electrostatic interactions and making five hydrogen bonds with it. Lys22 and Arg120 are conserved in all known MurA and EPSP synthase sequences, whereas there is a lysine residue in EPSP synthase corresponding to MurA Arg397. The shape of this phosphonate-binding site and the geometry of specific interactions suggest that the phosphate group of the natural substrate, PEP, also binds to this site. The arrangement of the arginine residues around the phosphate site is different from the geometry of interactions suggested by Li and co-workers [26]. In their time-resolved solid state NMR spectroscopy study of MurA from *E. cloacae* they predicted side-by-side interactions of a non-specific arginine with PEP, involving the internal nitrogen atom of the guanidino group.

Near the thioether bond with Cys115, there is a pocket between the fosfomycin carbon atom C-3 and two arginines (Arg331 and Arg371) that contains two water molecules. The arrangement of the arginine sidechains strongly suggests this pocket to be a binding site for the carboxylate group of PEP, particularly because the arginines are conserved in structure-based alignment of other MurA and EPSP synthase sequences. The fosfomycin-MurA structure, therefore, provides a good starting point for modelling PEP in its covalently bound form and for modelling other enzyme-bound intermediates of the reaction mechanism.

Conformational change upon binding substrate

Two observations suggest that MurA undergoes a conformational change during catalysis. Firstly, in the present structure, only the uridinyl and ribose rings of UDP-GlcNAc are exposed to solvent, so the domains must move apart for substrates to enter and products to leave. Secondly, the EPSP synthase structure suggests an alternative conformation for apo-MurA. From modelling studies of the MurA structure in its open conformation, we predict that, in addition to changes in the relative disposition of the two domains, the conformation of the loop 111–121 will be altered upon substrate-binding. We propose that the active site is created by induced fit following initial recognition and binding of UDP-GlcNAc, which in turn triggers a conformational change of the 111–121 loop, bringing Cys115 and PEP into place for reaction. This prediction is supported by the observation that time-dependent inactivation of MurA by fosfomycin is greatly accelerated by UDP-GlcNAc and also by unreactive 3′-deoxy-UDP-GlcNAc [24], implying that the binding of each influences a conformation change which facilitates the reaction of Cys115 with fosfomycin. The model also predicts that, in the open conformation, the contribution of Arg397 to the phosphate-binding site and to the salt-bridge with Asp49 would no longer be possible. This salt bridge is positioned between

the active site and the bulk solvent. Disruption resulting from some rearrangement of charge distribution during the final stage of the reaction would provide an opening to the active site, thereby allowing inorganic phosphate to leave and a molecule of PEP to gain access. Structure-based sequence alignment suggests that Asp49 and Lys411 would form a similar salt bridge in EPSP synthase.

Catalytic residues

The involvement of Cys115 in catalysis was established by site-directed mutagenesis studies: the substitution of this residue with serine or alanine results in an inactive enzyme [21,27]. However, Cys115 is replaced by an aspartate residue in the sequence of a gene from *M. tuberculosis* with 45% identity to the *E. coli* MurA gene (KE Kempsell and KD, unpublished data). This observation prompted a recent study into the consequence of aspartate substitution in *E. coli* MurA, which revealed that the mutated enzyme is highly active but resistant to inactivation by fosfomycin [23]. The results of this study imply that the cysteine or aspartate residue at position 115 performs the role of a general acid in the protonation of C-3 of PEP during the reaction. The crystal structure confirms that Cys115 is suitably positioned to play this role (Figs 3,5). The properties of this cysteine may be modulated by the relative disposition of certain charged sidechains in the catalytic site and by their movement during various stages of the reaction. For instance, the guanidinium moieties of Arg120 and Arg397 (conserved in all sequences) are close to Cys115, being 4.4 Å and 3.4 Å from the sulphur atom, respectively. Structure-based sequence alignment suggests that Glu118 in EPSP synthase, which corresponds to Gly114 in MurA, may have the catalytic role of Cys115. This hypothesis is supported by the observation that replacement of Cys115 in MurA with glutamate also yields an active enzyme, albeit with 1% of the activity of the aspartate mutant [23]. Two charged residues close to Glu118 in EPSP synthase (Lys122 and Glu123) could be involved in modifying the acid-base properties of the glutamate.

The role of the covalently bound PEP in MurA catalysis is unclear, as recent data prove that it is not required for catalysis and that non-covalently bound PEP is the species that reacts with UDP-GlcNAc [19,23]. Modelling suggests that the catalytic Cys115 is likely to be exposed to solvent in the open form of the enzyme. One possible function of this covalent bond may be to protect the cysteine from oxidation and from cross-linking with other cysteine-containing protein molecules. A thioester group in the human complement component C-4 has a similar function, keeping the acyl group ready for activation and protecting the thiol group from oxidation [28].

A candidate for the role of base in the initial deprotonation of the UDP-GlcNAc C-3 hydroxyl is Asp305 (Figs 3,4a). This residue makes two hydrogen bonds with the sugar ring, including a bond with the C-3 hydroxyl (2.9 Å). Rearrangements in this region during the formation of the tetrahedral intermediate may facilitate the conformational change leading to the release of the products at the final stage of the reaction. An aspartate residue at the structurally equivalent position 313 is conserved in all known sequences of EPSP synthase [27].

Biological implications

Antibiotics acting at different stages in the pathway leading to formation and assembly of bacterial peptidoglycan have been in clinical use for several decades. However, the emergence of drug-resistant bacteria has highlighted the need to continue to develop new classes of drugs. This has stimulated interest in the essential cytoplasmic enzymes that synthesise the key intermediate in peptidoglycan synthesis, UDP-*N*-acetylmuramyl pentapeptide. The first step in this process is the formation of UDP-*N*-acetylenolpyruvylglucosamine from phosphoenolpyruvate (PEP) and UDP-*N*-acetylglucosamine (UDP-GlcNAc), a reaction catalysed by UDP-*N*-acetylglucosamine enolpyruvyl transferase (MurA). Inhibitors of enolpyruvyl transferases are of potential commercial interest, because the only two known examples of this enzyme class, MurA and 5-enolpyruvylshikimate-3-phosphate (EPSP) synthase, are found exclusively in plants and microbes. The discovery of fosfomycin and glyphosate, as specific inhibitors of MurA and EPSP synthase, respectively, has highlighted this potential and also provided a means to confirm the previously determined catalytic mechanisms of the two enzymes. Interestingly, although both inhibitors were thought to compete with PEP, each did not inhibit both enzymes and it was concluded that the reactions were catalysed in different ways. More recently, gene sequencing and refined biochemical studies have shown that the enzymes and their mechanism are indeed related, and this is further supported by close structural similarity.

The structure of MurA complexed with substrate (UDP-GlcNAc) and inhibitor (fosfomycin), has the same overall protein fold as EPSP synthase, with two globular domains and the catalytic site situated in a cavity between the domains. However, the relative orientation of the domains is different in the two structures; the substrate-free form of EPSP synthase is in an 'open' conformation, whereas MurA is in a 'closed' conformation. The substrate and the inhibitor are bound in a deep active-site cavity interacting with residues from both domains. Fosfomycin is covalently-bound to the catalytic cysteine residue and can serve as a model for the covalently-bound form of PEP.

The high-resolution structure of MurA provides a wealth of information on the residues involved in MurA substrate binding and catalysis and gives a firm base for detailed

predictions of corresponding residues in EPSP synthase. It thus provides a template upon which novel inhibitors of this important enzyme class may be designed.

Materials and methods

Expression, purification and crystallization

E. coli MurA was isolated from the overproducing strain JLM16, with the following modifications from the method described previously [8]. After lysing the cells and centrifuging at low speed to remove cell debris, the extract was clarified by centrifugation at 100 000 × g for 2 h at 4° C, then dialyzed overnight against 50 mM TRIS.HCl, pH 8.0, 2 mM dithiothreitol. The ammonium sulphate step was omitted. Following chromatography of this material on Hi-Load Q Sepharose (Pharmacia), pooled active fractions were concentrated by ultrafiltration (Amicon PM30 membrane) to ~50 ml and applied to a 2L Superdex G75 (Pharmacia) gel filtration column (102 cm × 5 cm). Purified MurA was eluted in 50 mM TRIS.HCl, pH 8.0, 150 mM NaCl, 2 mM dithiothreitol. Purity was routinely assessed by sodium dodecyl sulphate polyacrylamide gel electrophoresis and by liquid chromatography and mass spectroscopy.

Crystals were grown using the sitting-drop vapour-diffusion method from a solution of ~10 mg ml^{-1} of protein, 2.5 mM UDP-GlcNAc and 2.5 mM fosfomycin, mixed with reservoir solution containing 25 % *tert*-butanol, 100 mM $CaCl_2$, 10 % glycerol and 100 mM TRIS buffer, pH 8.5. The enzyme crystallized in space group P321 with one molecule in the asymmetric unit. The cell dimensions are: a = 110.7 Å, c = 67.6 Å.

Data collection and processing

The X-ray data for the native crystals (2.8 Å resolution) and for the heavy-atom derivatives were collected on an Enraf-Nonius FAST area detector, mounted on a rotating-anode X-ray generator. The crystals were harvested from their original drops to a solution containing 40% *tert*-butanol, 10 % glycerol, 100 mM $CaCl_2$, 100 mM TRIS buffer, pH 8.5, and, for heavy-atom soaks, an appropriate heavy-atom compound. The crystals used for data collection were then briefly soaked in corresponding solutions, with glycerol concentration raised to 20 %, and flash-frozen at 100 K in a stream of dry nitrogen, using the Cryostream system (Oxford Cryosystems). Data processing was carried out using the program MADNES [29] and programs from the CCP4 suite [30]. The native X-ray data to 1.8 Å resolution were collected from one cryocooled crystal on station 9.6 at the synchrotron radiation source at Daresbury, using a MAR-research image plate and processed using MOSFLM [31].

Structure determination and refinement

The structure of MurA was solved by the method of multiple isomorphous replacement (MIR) using three different platinum derivatives: chloro (2,2′:6′2″-terpyridine) platinum (II) (data sets TP10 and TP25), potassium hexachloroplatinate (PTCL) and potassium tetrachloroplatinate (PT04) (Table 1). Atomic coordinates of the platinum atom of the PTCL derivative were found using the direct methods program SHELX [32], and refined with the phase refinement program MLPHARE [30]. Single isomorphous replacement phases computed from this derivative were used to calculate difference Fourier maps that revealed coordinates of the heavy-atom sites for the other derivatives. Several cycles of phase refinement were performed giving the final overall figure of merit of 0.47 for data between 20.0–3.2 Å for the four derivatives. Data sets TP10 and TP25 were collected from crystals soaked in the same heavy-atom compound solution, at different concentrations and for different lengths of time. As the relative occupancy of the common sites appeared to be significantly different, we included both data sets in the phasing, treating them as different derivatives. Binding of the heavy-atom compounds was examined later by calculating difference maps phased with the refined protein coordinates. The PTCL binding site was found to be close to the methionine residue Met366, the PT04 site is situated near Met1, three of the four TP10 sites are close to external histidine residues (His155, His285 and His344), and one TP10 binding site was found in the proximity of the exposed cysteine residue Cys81.

Figure 6

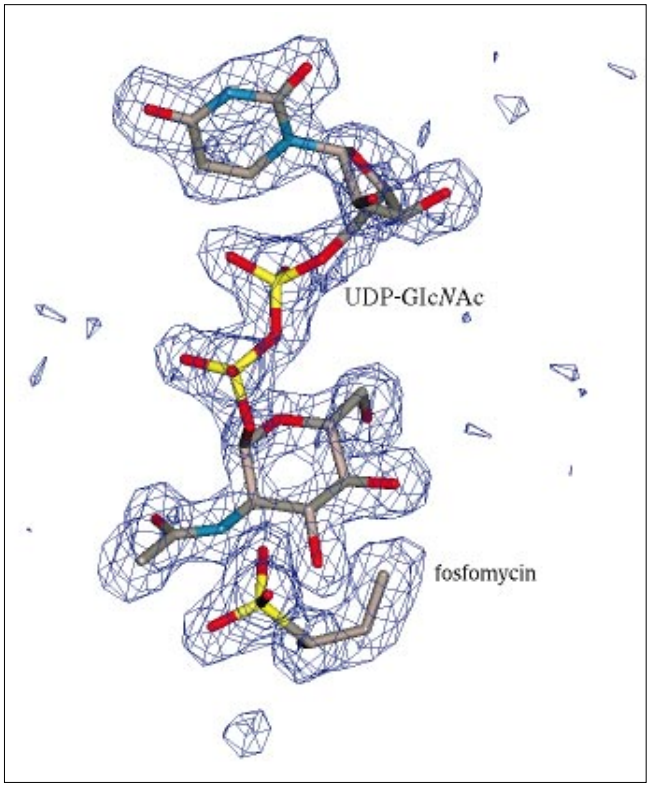

The difference electron density corresponding to UDP-GlcNAc and fosfomycin bound to the active site of MurA. The map is calculated at 1.8 Å resolution. Atoms are shown in standard colours. Figure was produced with the program QUANTA (Molecular Simulations Inc.).

The TP25 (lower concentration of the platinum compound) sites were close to Cys81 and His155 with the relative levels of electron density different from the corresponding sites of TP10.

The electron-density map at 3.2 Å resolution calculated using the MIR phases was noisy but it clearly showed the outline of the protein molecules in the unit cell and their similarity to the structure of EPSP synthase [15] with the pseudo-symmetrical arrangement of helices within the molecules. The quality of the map was greatly improved by the solvent-flattening procedure using the program DM [30], although several mainchain discontinuities remained, and some regions of the map were still poorly defined. Initial interpretation of the map was helped by using the α-carbon co-ordinates of the EPSP synthase structure. A model of the mainchain fold of MurA, based on fragments of the α-carbon co-ordinates of EPSP synthase (PDB entry code 1EPS), was fitted into the solvent-flattened MIR map using the program FRODO [33], and used to create a molecular mask for subsequent density-modification and phase combination procedures performed using programs from the CCP4 suite. This further improved the quality of the map and enabled interpretation of most of the electron density. Rounds of model building, density modification, phase combination and phase extension were performed resulting in fitting the complete polypeptide chain except for the disordered, C-terminal residue Glu419. The R_{free} indicator [34] was used to monitor the progress of the structure determination until it reached a value of 0.245 for 1.8 Å resolution data. It was not used in the final round of the refinement, which was based on all reflections. Automatic Refinement Program (ARP) [35], used during final stages of model building, proved invaluable in removing model bias and allowing correction of several mistakes made in the initial

Figure 7

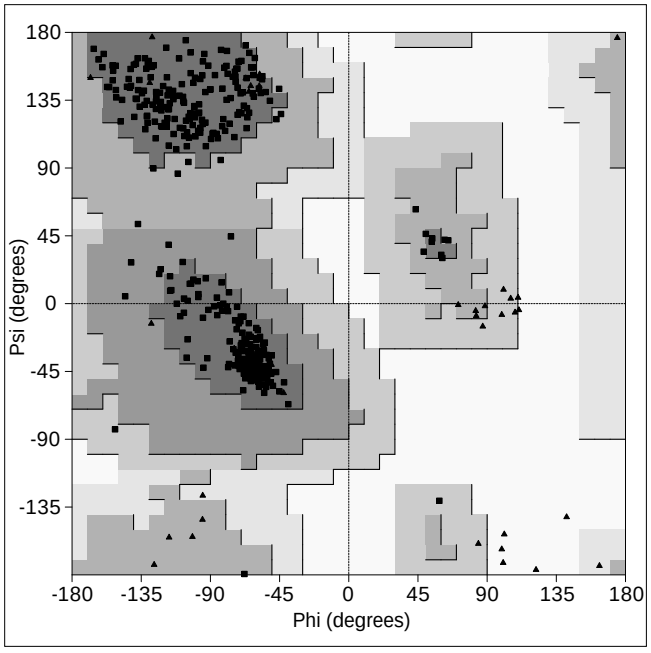

Ramachandran plot for the refined structure of MurA. Glycines are represented as triangles. Squares represent all the other residues. The plot was produced using the program PROCHECK [30].

interpretation. For example, an electron-density map resulting from the ARP procedure showed that a long segment of the polypeptide chain on the surface of the molecule (residues 320–370) contained amino-acid segments that were shifted by up to eight residues from their true positions. Correct positions were indicated by the shape of sidechain electron density. Difference electron density corresponding to UDP-GlcNAc and fosfomycin, computed after the initial refinement of the protein, was very clear, and the atomic co-ordinates of both ligands were subsequently included in the model (Fig. 6).

The structure was initially refined using the program PROLSQ [36], and the program X-PLOR [37] was used at later stages. Several rounds of model rebuilding and structure refinement were performed at increasing resolution using the 1.8 Å data set until convergence was reached, with the final crystallographic R factor of 0.185 for all 40374 reflections in the 6.0–1.8 Å resolution range. The root mean square (rms) deviations of bond lengths and angles from stereochemical standards were 0.018 Å and 2.85° respectively. The final difference electron-density map was devoid of any features significantly higher than noise level. The model has been examined using the program PROCHECK [30]. It shows good geometry (Fig. 7), with 93.6 % residues having the ϕ/ψ torsion angles in the most favoured region of the Ramachandran diagram, 5.8 % in additional allowed regions, 0.6 % (two residues) in generously allowed regions, and no residues in disallowed regions of the diagram.

Accession numbers

The atomic coordinates for MurA have been deposited in the Brookhaven Protein Data Bank with the code number 1UAE.

Note added in proof

The structure of an *apo* form of MurA from highly homologous *Enterobacter cloacae* was published recently (Schönbrunn, E., *et al.*, & Mandelkow, E. (1996). Crystal structure of UDP-*N*-acetylglucosamine enolpyruvyltransferase the target of the antibiotic fosfomycin. *Structure* **4**, 1065–1075). It confirms our hypothesis regarding the conformation changes that take place during catalysis.

Acknowledgements

We thank Albert Jaxa-Chamiec, Janette Thomas, Mike Hann, Watson Lees, Dennis Kim and Christopher Walsh for useful discussions during the course of this work.

References

1. Bugg, T.D.H. & Walsh, C.T. (1992). Intracellular steps of bacterial cell wall peptidoglycan biosynthesis: enzymology, antibiotics, and antibiotic resistance. Nat. Prod. Rep. **1992**, 199–215.
2. Hendlin, D., *et al*., & Mata, J.M. (1969). Phosphomycin, a new antibiotic produced by strains of *Streptomyces. Science* **166**, 122–123.
3. Kahan, F.M., Kahan, J.S., Cassidy, P.J. & Kropp, H. (1974). The mechanism of action of fosfomycin (phosphonomycin). *Ann. N.Y. Acad. Sci.* **235**, 364–386.
4. Benson, T.E., Filman, D.J., Walsh, C.T. & Hogle, J.M. (1995). An enzyme-substrate complex involved in bacterial cell wall biosynthesis. *Nat. Struct. Biol.* **2**, 644–653.
5. Fan, C., Moews, P. C., Walsh, C. T. & Knox, J. R. (1994). Vancomycin resistance: Structure of D-alanine: D-alanine ligase at 2.3 Å resolution. *Science* **266**, 439–443.
6. Jin, H. Y., *et al*., & Villafranca, J.J. (1996). Structural studies of *Escherichia coli* UDP-*N*-acetylmuramate-L-alanine ligase. *Biochemistry* **35**, 1423–1431.
7. Wanke, C., Falchetto, R. & Amrhein, N. (1992). The UDP-*N*-acetylglucosamine 1-carboxyvinyl transferase of *Enterobacter cloacae. FEBS Lett.* **301**, 271–276.
8. Marquardt, J.L., Siegele, D.A., Kolter, R. and Walsh, C.T. (1992). Cloning and sequencing of *Escherichia coli MurZ* and purification of its product, a UDP-*N*-acetylglucosamine enolpyruvyl transferase. *J. Bacteriol.* **174**, 5748–5752.
9. Gonzalez-y-Marchand, J.A., Colston, M.J. & Cox, R.A. (1996). The rRNA operons of *Mycobacterium smegmatis* and *Mycobacterium tuberculosis:* comparison of promoter elements and of neighbouring upstream genes. *Microbiology* **142**, 667–674.
10. Sela, S. & Clark-Curtiss, J.E. (1991). Cloning and characterization of the *Mycobacterium leprae* putative ribosomal RNA promoter in *Escherichia coli*. *Gene* **98**, 123–127.
11. Fleischmann, R.D., *et al*., & Venter, J.C. (1995). Whole-genome random sequencing and assembly of *Haemophilus influenzae Rd*. *Science* **269**, 496–512.
12. Trach, K., *et al*., & Hoch, J.A. (1988). Complete sequence and transcriptional analysis of the spoOF region of the *Bacillus subtilis* chromosome. *J. Bacteriol.* **170**, 4194–4208.
13. Ehrt. S. & Hillen, W. (1994). UDP-*N*-acetylglucosamine 1-carboxyvinyl transferase from *Acinetobacter calcoaceticus*. *FEMS Microbiol. Lett.* **117**, 137–142.
14. Duncan, K., Lewendon, A. & Coggins, J.R. (1984). The complete amino acid sequence of *Escherichia coli* 5-enolpyruvylshikimate 3-phosphate synthase. *FEBS Lett.* **170**, 59–63.
15. Stallings, W.C., *et al*., & Kishore, G.M. (1991). Structure and topological symmetry of the glyphosate target 5-enol pyruvylshikimate-3-phosphate synthase: a distinctive protein fold. *Proc. Natl. Acad. Sci. USA* **88**, 5046–5050.
16. Marquardt, J.L., Brown, E.D., Walsh, C.T. & Anderson, K.S. (1993). Isolation and structural elucidation of a tetrahedral intermediate in the UDP-*N*-acetylglucosamine enolpyruvoyl transferase enzymatic pathway. *J. Am. Chem. Soc.* **115**, 10398–10399.
17. Bondinell, W.E., Vnek, J., Knowles, P.F., Sprecher, M. & Sprinson, D.B. (1971). On the mechanism of 5-enolpyruvylshikimate 3-phosphate synthetase. *J. Biol. Chem.* **246**, 6191-6196.
18. Anderson, K.S. & Johnson, K.A. (1990). Kinetic and structural analysis of enzyme intermediates: lessons from EPSP synthase. *Chem. Rev.* **90**, 1131–1149.
19. Kim, D.H., Tucker-Kellogg, G.W., Lees, W.J. & Walsh, C.T. (1996). Analysis of fluoromethyl group chirality establishes a common stereochemical course for the enolpyruvyl transfers catalyzed by EPSP synthase and UDP-GlcNAc enolpyruvyl transferase. *Biochemistry* **35**, 5435–5440.
20. Cassidy, P.J. & Kahan, F.M. (1973). A stable enzyme-phosphoenolpyruvate intermediate in the synthesis of uridine-5′-diphospho-*N*-acetyl-2-amino-2-deoxyglucose 3-*O*-enolpyruvyl ether. *Biochemistry* **12**, 1364–1373.

21. Wanke, C. & Amrhein, N. (1993). Evidence that the reaction of UDP-*N*-acetylglucosamine 1-carboxyvinyltransferase proceeds through the *O*-phosphothioketal of pyruvic acid bound to Cys115 of the enzyme. *Eur. J. Biochem*. 218, 861–870.
22. Brown, E.D., Marquardt, J.L., Lee, J.P., Walsh, C.T. & Anderson, K.S. (1994). Detection and characterisation of a phospholactyl-enzyme adduct in the reaction catalyzed by UDP-*N*-acetylglucosamine enolpyruvyl transferase, MurZ. *Biochemistry* 33 10638–10645.
23. Kim, D.H., Lees, W.J., Kempsell, K.E., Lane, W.S., Duncan, K. & Walsh, C.T. (1996). Characterization of a Cys115 to aspartate substitution in the *Escherichia coli* cell wall biosynthetic enzyme UDP-GlcNAc enolpyruvyl transferase (MurA) that confers resistance to inactivation by the antibiotic fosfomycin. *Biochemistry* 35, 4923–4928.
24. Marquardt, J.L., *et al*., & Walsh, C. (1994). Kinetics, stoichiometry, and identification of the reactive thiolate in the inactivation of UDP-GlcNAc enolpyruvoyl transferase by the antibiotic fosfomycin. *Biochemistry* 33, 10646–10651.
25. Steinrücken, H.C. & Amrhein, N. (1980). The herbicide glyphosate is a potent inhibitor of 5-enolpyruvyl-shikimic acid-3-phosphate synthase. *Biochem. Biophys. Res. Commun*. 94, 1207–1212.
26. Li, Y., Krekel, F., Ramilo, C., Amrhein, N. & Evans J.N.S. (1995). Time-resolved solid-state REDOR NMR studies of UDP *N*-acetylglucosamine enolpyruvyl transferase. *FEBS Lett*. 95, 208–212.
27. Marquardt, J.L. (1993). Molecular studies of the enzymes involved in UDP-*N*-acetylmuramic acid biosynthesis. PhD Thesis, Department of Biological Chemistry and Molecular Pharmacology, Harvard University.
28. Dods, A.W., Ren, X-D., Willis, A.C. & Law, S.K.A. (1996). The reaction mechanism of the internal thioester in the human complement component C4. *Nature* 379, 177–179.
29. Messerschmidt, A. & Pflugrath, J.J. (1987). Crystal orientation and X-ray pattern prediction routines for area detector diffractometer systems in macromolecular crystallography. *J. Appl. Cryst.* 20, 306–315.
30. Collaborative Computational Project, No. 4, (1994). The CCP4 Suite: programs for protein crystallography *Acta Cryst*. *D* 50, 760–763.
31. Leslie, A.G.W., Brick, P. & Wonacott, A.J. (1986). MOSFLM. Daresbury Laboratory Information Quarterly. *Protein Cryst*. 18, 33–39
32. Sheldrick, G.M. (1985). SHELX-84. In *Crystallographic computing 3: Data collection, structure determination, proteins, and databases*. (Sheldrick G.M., Krüger, C. & Goddard, R., eds), pp. 184–189, Clarendon Press, Oxford, UK.
33. Jones, T.A. (1985). Interactive computer graphics: FRODO. *Methods Enzymol.* 115, 157–171.
34. Brünger, A.T. (1992). Free R value, a novel statistical quantity for assessing the accuracy of crystal structures. *Nature* 355, 472–475.
35. Lamzin, V.S. & Wilson, K.S. (1993). Automated refinement of protein models. *Acta Cryst. D* 49, 129–147.
36. Hendrickson, W.A., (1985). Stereochemically restrained refinement of macromolecular structures. *Methods Enzymol*. 115, 252–271.
37. Brünger, A.T., Kuriyan, J. & Karplus, M. (1987). Crystallographic R factor refinement by molecular dynamics. *Science* 235, 458–460.
38. Kraulis, P.J. (1991). MOLSCRIPT: a program to produce both detailed and schematic plots of protein structures. *J. Appl. Cryst.* 24, 946–950.
39. Bacon, D.J. & Anderson, W.F. (1988). A fast algorithm for rendering space-filling molecule pictures. *J. Mol. Graph.* 6, 219–220.
40. Merritt, E.A. & Murphy, M.E.P. (1994). Raster3D, Version 2.0 - A program for photorealistic molecular graphics. *Acta Cryst. D* 50, 869–873.